BIOCHEMISTRY
including biophysical chemistry & molecular biology

Article

pubs.acs.org/biochemistry

Kinetic and Thermodynamic Features Reveal That *Escherichia coli* BCP Is an Unusually Versatile Peroxiredoxin

Stacy A. Reeves, Derek Parsonage, Kimberly J. Nelson, and Leslie B. Poole*

Department of Biochemistry, Wake Forest School of Medicine, Winston-Salem, North Carolina 27157, United States

Supporting Information

ABSTRACT: In *Escherichia coli*, bacterioferritin comigratory protein (BCP) is a peroxiredoxin (Prx) that catalyzes the reduction of H_2O_2 and organic hydroperoxides. This protein, along with plant PrxQ, is a founding member of one of the least studied subfamilies of Prxs. Recent structural data have suggested that proteins in the BCP/PrxQ group can exist as monomers or dimers; we report here that, by analytical ultracentrifugation, both oxidized and reduced *E. coli* BCP behave as monomers in solution at concentrations as high as 200 μM. Unexpectedly, thioredoxin (Trx1)-dependent peroxidase assays conducted by stopped-flow spectroscopy demonstrated that $V_{max,app}$ increases with increasing Trx1 concentrations, indicating a nonsaturable interaction (K_m > 100 μM). At a physiologically reasonable Trx1 concentration of 10 μM, the apparent K_m value for H_2O_2 is ~80 μM, and overall, the V_{max}/K_m for H_2O_2, which remains constant at the various Trx1 concentrations (consistent with a ping-pong mechanism), is ~1.3×10^4 M^{-1} s^{-1}. Our kinetic analyses demonstrated that BCP can utilize a variety of reducing substrates, including Trx1, Trx2, Grx1, and Grx3. BCP exhibited a high redox potential of −145.9 ± 3.2 mV, the highest to date observed for a Prx. Moreover, BCP exhibited a broad peroxide specificity, with comparable rates for H_2O_2 and cumene hydroperoxide. We determined a pK_a of ~5.8 for the peroxidatic cysteine (Cys45) using both spectroscopic and activity titration data. These findings support an important role for BCP in interacting with multiple substrates and remaining active under highly oxidizing cellular conditions, potentially serving as a defense enzyme of last resort.

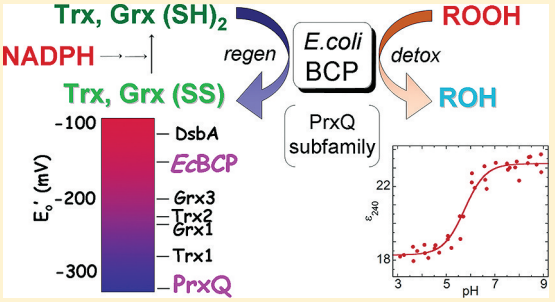

Like all aerobic bacteria, *Escherichia coli* must cope with damaging endogenous sources of reactive oxygen species (ROS) that result from autoxidation of components of the aerobic respiratory chain and byproducts of reactions with ferrous iron (Fenton chemistry).[1] In addition, *E. coli* is exposed to endogenous ROS released from other bacteria to ward off noncommensal intruders as well as from macrophages and neutrophils, which release ROS as part of their microbicidal arsenals.[2−4] In response, *E. coli* employs a variety of antioxidant defense mechanisms, including proteins such as superoxide dismutase and catalase and small molecules such as glutathione. Included among the defenses are a number of proteins that detoxify hydrogen peroxide and/or organic hydroperoxides, including KatG (HPI) and HPII (cytosolic and periplasmic catalases, respectively), BtuE (a glutathione peroxidase homologue), and three distinct members of the peroxiredoxin (Prx) family.[5]

Prxs are fundamentally important, strongly expressed, cysteine-dependent peroxidases found in nearly all organisms. Unlike catalase, which converts H_2O_2 to H_2O and O_2, Prxs convert H_2O_2 into two H_2O molecules with the reducing equivalents ultimately coming from NADPH or NADH. In all Prxs, the active site (or peroxidatic) Cys (denoted C_p) is located within a conserved (PXXXTXXC$_p$) motif.[6] This active site Cys reacts with hydroperoxide substrates to generate a sulfenic acid (R-SOH). In many Prxs, a second Cys (the so-called resolving Cys, denoted C_r) reacts with the sulfenic acid to form a disulfide bond that prevents further damaging oxidation of the C_p and provides an accessible, disulfide-bonded substrate for recycling by Trx or Trx-like redoxins.[7−9] Multiple Prxs are often expressed in a given organism, yet they cannot typically substitute for one another in knockout experiments. In eukaryotes, the role of Prxs clearly extends beyond simple detoxification into complex phenomena such as the regulation of cell signaling, resistance toward radiation treatment, and tumor suppression, though precise roles and mechanisms of these aspects are a major area of research in this field.[10−14]

E. coli contains three Prxs from three different subfamilies: AhpC (Prx1/AhpC subfamily), Tpx (Tpx subfamily), and BCP (also known as bacterioferritin comigratory protein) from the BCP/PrxQ subfamily.[6] AhpC is highly reactive with H_2O_2, with a k_{cat}/K_m of 1.4×10^7 M^{-1} s^{-1}. Although it is also able to reduce bulkier hydroperoxide substrates, the K_m values for cumene hydroperoxide (CHP, 107 μM) and *tert*-butyl hydroperoxide (*t*BHP, 238 μM) are significantly higher than that for H_2O_2 (1.4 μM).[15] AhpC and other Prx1/AhpC subfamily members form homodimers across the β-sheet-extending B-type interface, and these dimers further oligomerize into decamers across the A-type interface (for "ancestral" or "alternate") in a redox-

Received: June 17, 2011
Revised: September 11, 2011
Published: September 12, 2011

sensitive and concentration-dependent manner.[16−18] Reduced AhpC is present as a decamer, whereas disulfide-bonded AhpC can dissociate into dimers at lower protein concentrations.[18] AhpF, the specialized reductant for AhpC, accepts electrons from NADH and delivers them to AhpC through three redox centers (FAD and two redox-active disulfide centers) within tethered Trx reductase-like and Trx-like domains.[9,19] In contrast, *E. coli* Tpx preferentially reduces the bulkier hydroperoxide, CHP [k_{cat}/K_m (for peroxide) = 7.7 × 10^6 M^{-1} s^{-1}], compared with H_2O_2 (k_{cat}/K_m = 4.4 × 10^4 M^{-1} s^{-1}) and forms stable dimers across the A-type interface in a non-redox-sensitive manner.[5] Previous studies have shown that *E. coli* Tpx is reduced by NADPH through thioredoxin reductase and Trx1 and cannot be reduced by Trx2, Grx1, or AhpF.[5]

Much less is known about the substrates and function of BCP, the third *E. coli* Prx family member. The BCP/PrxQ subfamily is one of the least characterized Prx subfamilies overall that nonetheless is present across archaea, bacteria, and some eukaryotic organisms, including plants and *Caenorhabditis elegans*.[6,20,21] Bioinformatic analyses of Prxs have been facilitated recently by the increasing amount of structural and sequence information available for these proteins, and various studies have suggested that members of the BCP subfamily are most similar to the ancestral Prx protein.[6,17,22] Within the BCP/PrxQ subfamily of proteins, the low-potential PrxQ proteins of plant chloroplasts have been studied by several groups and have been shown to be important in maintaining photosynthesis within this organelle.[23] *E. coli* BCP reportedly exhibits low peroxidase activity with Trx1, raising the question of whether this protein might be more active with other peroxide or reducing substrates.[24] The functional importance of this protein has been demonstrated, at least in the human pathogen *Helicobacter pylori*, where it helps establish long-term infections within the host's gastric mucosa.[25]

Interestingly, the C_r residue has been found in at least four different locations across all Prxs (in helices α2, α3, and α5 and the C-terminal tail) and can involve either an intrasubunit or intersubunit linkage.[17,22] The presence of a C_r is particularly variable in the BCP/PrxQ subfamily,[6] with members possessing a C_r in helix α2 (54%)[26,27] or α3 (like members of the Tpx subfamily, 7%)[28] or lacking a C_r altogether (≤39%). In cases where C_r is missing (in the so-called "1-Cys" enzymes), less is understood about the reductive recycling pathways, but small molecule thiols like glutathione or thiol groups from other proteins like redoxins may be involved.[6,29] *E. coli* BCP is representative of the largest group of BCP/PrxQ proteins, with the C_r located five residues after the C_p in helix α2.[22,26] Reports to date have concluded that *E. coli* BCP is a monomeric protein, although the recent finding that BCP/PrxQ subfamily members can be dimeric suggests that more rigorous studies of the oligomeric state of this protein in solution are warranted.[17]

This study was designed to gather detailed information about the peroxidatic function and biochemical underpinnings of the reactivity of *E. coli* BCP. Its oligomeric and kinetic properties, substrate preferences (for both hydroperoxide and reducing substrates), redox potential, and pK_a for C_p were all investigated and found to support a broad substrate specificity and wide tolerance of varying cell conditions. For example, this enzyme is less dependent than the other two Prxs (AhpC and Tpx) on specific reducing pathways, which may be compromised under conditions that would render other oxidant defenses less active. As a high-potential redoxin, it is also poised to remain reduced under highly oxidizing conditions that would likely compromise other defense systems within the cell.

EXPERIMENTAL PROCEDURES

Cloning and Mutagenesis of BCP from *E. coli*. The BCP structural gene (GenBank accession number EU897604.1) was amplified by polymerase chain reaction (PCR) from *E. coli* XL1-Blue cells. The resulting PCR product was purified from an agarose gel using the QIAquick gel extraction kit (QIAGEN) and ligated into the pCR-Blunt-TOPO PCR cloning vector (Invitrogen) following the manufacturer's protocol. The sequence and orientation of the insert were confirmed by plasmid sequencing. The resulting plasmid was digested with *Eco*RI and *Bam*HI; the digested fragments were gel purified, and the BCP-encoding fragment was ligated into pTrc99A (Amersham Pharmacia Biotech Inc., Piscataway, NJ) to generate the wild-type BCP expression construct.

BCP mutagenesis (C45S, C50S, C99S, and C50S/C99S) was performed using the QuikChange II Site-Directed Mutagenesis Kit (Stratagene) following the manufacturer's protocol. All mutations were confirmed by sequencing of the entire BCP-encoding insert.

Protein Expression and Purification. For all protein preparations, cells were lysed by being passed through an Avestin EmulsiFlex-C5, and cell debris was removed by centrifugation at 40000*g* for 40 min. Purification procedures were conducted at 4 °C, unless indicated otherwise. All chromatography, unless noted otherwise, was accomplished using an Akta Explorer 10S Air FPLC system (GE Healthcare).

Wild-type *E. coli* BCP was expressed from TA4315 cells, which lack AhpC, the major Prx of *E. coli*;[30] all BCP mutants were expressed and purified from *E. coli* strain JW2465, from the Keio collection, which has a confirmed knockout in BCP.[31] Cells were grown at 37 °C in 6 L of LB medium containing 100 μg/mL ampicillin to an A_{600} of 0.6 and then induced for 18 h with 0.8 mM isopropyl 1-thio-β-D-galactopyranoside (IPTG). Cells were harvested and resuspended in 50 mM potassium phosphate with 1 mM EDTA at pH 7.0 (buffer A) and lysed as described above. The nucleic acids were removed from the cleared lysate by the addition of 1% (w/v) streptomycin sulfate and centrifugation at 18000*g* for 20 min. The resulting supernatant was applied to a Q-Sepharose HP (GE Healthcare) column equilibrated with buffer A and eluted using a linear gradient from 0 to 1.0 M NaCl. Fractions were pooled, concentrated, and loaded onto a 250 mL Superose 12 prep grade (GE Healthcare) gel filtration column equilibrated with buffer A (except lacking EDTA). Fractions were pooled and loaded onto a 10 mL CHT Ceramic Hydroxyapatite (Bio-Rad Laboratories) gravity-flow column equilibrated with 5 mM sodium phosphate (pH 7.0). The column was washed using a stepwise concentration gradient of 50 and 100 mM sodium phosphate, and BCP was eluted at 200 mM sodium phosphate. Fractions containing purified BCP (~180 mg) were pooled and stored as 10 mg/mL aliquots at −80 °C. Mutant BCP proteins were expressed and purified essentially as described for the wild type, except that 2 mM dithiothreitol (DTT) was present during all steps of the purification, as previously required to prevent oxidative damage for similar mutants of AhpC and Tpx lacking the resolving Cys.[5,32]

To obtain pure Trx1, W3110 cells containing pDL59ΔT4,[33] a Trx1-expressing, heat inducible plasmid, were grown at 30 °C in 6 L of 2×YT medium in the presence of ampicillin (100 μg/

mL) to an A_{600} of 0.6 and then grown at 42 °C for 18 h. Trx1 was purified as previously described,[34] except that the crude extract was heated at 65 °C for 20 min and then centrifuged before being subjected to chromatography with Q-Sepharose HP and Superose 12 prep grade columns. Purity was verified by SDS−polyacrylamide gels, and pure Trx1 was concentrated and stored as 10 mg/mL aliquots at −80 °C.

Grx1 was expressed with a removable, N-terminal His tag in *E. coli* BL21(DE3) and purified as described previously.[35] Briefly, the fusion protein was purified on a HiTrap Chelating HP column (GE Healthcare), cleaved with thrombin, and applied to a Superose 12 prep grade column. The F6W mutant of Grx1 ($Grx1_{F6W}$) was expressed and purified from *E. coli* C41(DE3) cells as previously described.[36]

Trx2 with an N-terminal His tag was expressed in DHB4 *E. coli* cells transformed with plasmid DR1000 containing *trxC* in a pET15b vector.[37] Cells were grown at 37 °C to an A_{600} of 0.6 and induced with 0.8 mM IPTG for 18 h. The Trx2 protein was purified and the His tag removed essentially as described above for Grx1.

Grx3 was expressed from pRO1 (*grxC* in a pBAD33-derived plasmid)[38] harbored within DHB4 *E. coli* and purified using previously described methods.[39,40] Briefly, 6 L of cell culture induced for protein expression by addition of 0.02% arabinose was harvested, lysed, and treated with streptomycin sulfate. Chromatographic separations used Q-Sepharose (equilibrated and eluted with increasing NaCl in buffer A, except at pH 8) and Superose 12 columns (also using buffer A at pH 8).

Expression of DsbA from *E. coli* XL1-Blue transformed with pBJ41[41] was induced by overnight growth at 37 °C after addition of 1 mM IPTG when A_{600} equaled 1. The harvested cells were treated with 300 μg/mL lysozyme in buffer containing 20% sucrose, 20 mM Tris-HCl (pH 8.0), and 2.5 mM EDTA. The resulting supernatant after centrifugation was dialyzed against 10 mM Tris-HCl containing 0.25 mM EDTA (pH 8.0), loaded onto a 55 mL Q-Sepharose HP column equilibrated with the same buffer, and eluted with a 0 to 0.5 M NaCl gradient. Peak fractions containing DsbA were pooled, brought to 1 M in ammonium sulfate, and loaded onto a 75 mL Phenyl Sepharose HP column equilibrated with 1 M ammonium sulfate, 20 mM Tris-HCl (pH 8.0), and 0.1 M NaCl. DsbA was eluted using a 1 to 0 M ammonium sulfate gradient. Fractions containing pure protein were pooled, concentrated, and frozen in aliquots at 10 mg/mL.

E. coli thioredoxin reductase (TrxR) was purified as previously described.[19] Yeast glutathione reductase was purchased from Sigma.

Analytical Ultracentrifugation. Multiple concentrations of both oxidized and reduced BCP (25, 33, 50 66, 100, and 200 μM) were analyzed by sedimentation velocity experiments using an Optima XL-A analytical ultracentrifuge (Beckman Instruments, Palo Alto, CA) outfitted with absorbance optics. Before analysis, BCP was treated with 10 mM DTT for 30−60 min, DTT was removed, and the buffer was exchanged using a PD10 (GE Healthcare) column (reduced BCP sample). Oxidized BCP was prepared from the freshly reduced protein by addition of 10 mM H_2O_2 for 5 min and exchanged into fresh buffer without H_2O_2 using a PD10 column. Samples were analyzed at 20 °C in double-sectored cells in 25 mM potassium phosphate buffer, 1 mM EDTA, and 0.15 M NaCl (pH 7); reduced BCP buffers also contained 0.1 mM DTT. Sedimentation data at 280 nm were collected every 4 min at a rotor speed of 42000 rpm and a radial step size of 0.003 cm. Values of 0.73445 and 0.73446 cm^3/g for the partial specific volumes of reduced and oxidized BCP, respectively, were calculated from their amino acid compositions.[42] The molecular weight was calculated using the Svedberg equation[43] after extrapolation to zero concentration of the corrected sedimentation coefficient ($s^0_{20,w}$) and the translational diffusion coefficient ($D^0_{20,w}$) obtained using SVEDBERG version 6.39 (www.jphilo.mailway.com).[44,45]

Kinetic Assays. Previous NADPH-dependent assays conducted by Jeong et al.[24] used a single concentration of Trx1 and amounts of BCP that were equivalent to or in excess of the amount of Trx1; under these conditions, BCP turnover is expected to be limited by the rate of reduction. We therefore adapted those assays to measure BCP's activity with various reductants so that each reductant was in at least a 10-fold excess over BCP. Reactions were conducted at 25 °C in buffer A containing 150 μM NADPH, 0.5 μM BCP, and 1 mM CHP; CHP rather than H_2O_2 was used because H_2O_2 gave a significant background rate of reaction with glutathione under these conditions, whereas CHP did not. Assays with 10 μM Trx1 or Trx2 contained 0.1 μM TrxR (control experiments with twice as much or half as much TrxR did not give different rates, confirming that this amount is in excess). Assays with 10 μM Grx1, $Grx1_{F6W}$, or Grx3 instead contained 1 mM glutathione and 1 unit/mL glutathione reductase. Assay mixtures were first prepared without CHP, monitored for 1−2 min to establish the low background rate, and then supplemented with CHP to start the BCP-dependent peroxidase reaction. A_{340} was followed for the first 2 min of the reaction on an Agilent 8453 diode array spectrophotometer, and initial linear rates were determined to calculate the rate of NADPH oxidation using an ε_{340} of 6220 M^{-1} cm^{-1}.

Bisubstrate kinetic analysis with varying Trx1 and hydrogen peroxide concentrations and studies that aimed to determine BCP specificity with H_2O_2, cumene hydroperoxide (CHP), or *tert*-butyl hydroperoxide (*t*BHP) with both Trx1 and Grx1 were performed using an Applied Photophysics SX.18MV stopped-flow spectrophotometer. First, Trx1 (or $Grx1_{F6W}$) and BCP were prereduced by 10 mM DTT for 1 h, and excess DTT was removed by using a PD10 size exclusion column (GE Healthcare). Previous assays conducted with these proteins have established that this treatment fully reduces the Trx proteins on the basis of the appearance of two free thiol groups after reduction (detected by addition of DTNB).[32,36,46] A similar test with Grx1 established that 2.06 thiol groups per polypeptide were also generated by this treatment (regardless of whether 4 M guanidine hydrochloride is included in the DTNB assay buffer) and were maintained for >5 h after removal of the DTT with a PD10 column. Prereduced BCP was mixed in one syringe with either Trx1 or Grx1 and the reaction buffer (buffer A, present in both syringes); peroxide was added to the second syringe. After the samples had been mixed, the rate of reaction was measured by monitoring the change in fluorescence of Trx as it is oxidized, with excitation at 280 nm and emission at >320 nm (using an emission filter). Initial rates for the fluorescence changes at each Trx or Grx concentration were converted to micromolar peroxide reduced per second per micromolar BCP using eq 1.

$$\text{rate}\ [\text{in}\ \mu\text{M peroxide}\ s^{-1}\ (\mu\text{M BCP})^{-1}] = \text{rate}\ (\text{in V}\ s^{-1}) \times \frac{[\text{reductant}]}{\Delta F[\text{BCP}]} \quad (1)$$

where [reductant] (Trx1 or $Grx1_{F6W}$) and [BCP] are the final micromolar concentrations and ΔF is the maximum reductant fluorescence signal change (in volts) in the presence of excess peroxide for the same reductant concentration as that being analyzed. Under these conditions, the contribution to the total fluorescence changes from the very minor BCP fluorescence changes as the redox state of this protein changes is negligible.[36]

The initial rate of fluorescence decrease was determined by linear regression of the data during the first 2 s of the reaction. Reported rates are averages of three measurements from no fewer than three independent assays conducted at 25 °C.

Determination of Midpoint Reduction (Redox) Potentials. Reduced BCP (50 μM) was mixed with oxidized DsbA (50 μM) in 100 mM potassium phosphate and 1 mM EDTA (pH 7.0) and allowed to equilibrate anaerobically for 6 h at room temperature (an equilibration time that was verified to be sufficient in preliminary experiments). Although we have previously used a rapid acidification of the sample followed by direct separation by high-performance liquid chromatography (HPLC), in this case an additional step of rapid alkylation with *N*-ethylmaleimide (NEM) had to be added to trap free thiol groups and improve separation on HPLC of the reduced and oxidized species of BCP in the same gradient in which the two redox forms of DsbA were resolved. Thus, samples (50 μL) were quenched by adding 50 μL of 200 mM NEM for 2 min, followed by addition of a 10% volume of 1 M phosphoric acid, and then aliquots were resolved using a 4.6 mm × 250 mm Vydac C4 HPLC column. Protein components were separated using a shallow gradient of acetonitrile (50 to 60% acetonitrile for 60 min and then 60 to 82% acetonitrile for an additional 102 min), with 0.08−0.1% trifluoroacetic acid in both solvents, at a flow rate of 0.5 mL/min and room temperature. The locations of the peaks for the reduced and oxidized species were determined using standards for each protein, and quantitation of the proteins was based on the peak area for each species. The redox potential was calculated by using a derivation of the Nernst equation (eq 2) and a value of −110 mV (range of −122 to −100 mV) for the DsbA redox potential.[47−49]

$$E_o'(\mathrm{BCP}) = E_o'(\mathrm{DsbA}) + (RT/nF)\ln\left(\frac{[\mathrm{DsbA_{ox}}][\mathrm{BCP_{red}}]}{[\mathrm{DsbA_{red}}][\mathrm{BCP_{ox}}]}\right) \quad (2)$$

In separate experiments, oxidized BCP was mixed with reduced DsbA and incubated for 12 and 24 h at room temperature to ensure complete equilibration of the two proteins.[15]

Stability and pK_a Analysis of BCP. The pK_a of BCP (wild type and mutant) was determined by measuring the change in the ε_{240} between pH 3 and 9, following confirmation that the protein was stable across this pH range (retained full activity when shifted back to pH 7), essentially as previously described.[32] For pK_a analysis, BCP was first reduced with 10 mM DTT for 10 min, and then excess DTT was removed using a PD10 column pre-equilibrated with 5 mM potassium phosphate and 1 mM EDTA (pH 7). The concentration of reduced BCP was determined using an ε_{280} of 15400 M^{-1} cm^{-1}. BCP was diluted to a final concentration of 25 μM into citrate-borate-phosphate (CBP) buffer containing each component at 10 mM (sodium citrate, boric acid, and sodium phosphate), 100 mM sodium chloride, and 0.1 mM diethylenetriaminepentaacetic acid (DTPA) at various pH values between 3 and 9; the final pH value of each solution was determined after mixing. At each pH, the absorbance values at 240 and 280 nm were measured with an Agilent 8453 diode array spectrophotometer and the ε_{240} was calculated assuming that the ε_{280} value remained constant across the pH range. The ε_{240} values were plotted versus pH, and the pK_a was determined by direct fit to eq 3:

$$y = [(A \times 10^{\mathrm{pH}}) + (B \times 10^{\mathrm{p}K_a})]/(10^{\mathrm{p}K_a} + 10^{\mathrm{pH}}) \quad (3)$$

where $y = \varepsilon_{240}$, A is the upper plateau at high pH (ε_{240} for the deprotonated form), and B is the lower plateau at low pH (ε_{240} for the protonated form).

The pK_a of BCP was also determined by measuring the pH dependence of BCP peroxidase activity. The rate of peroxide disappearance was measured using the FOX assay to assess peroxide levels.[50] Prereduced BCP was diluted to 40 μM in 2× CBP buffer at various pH values between 4.5 and 8, and the assay was started by the addition of an equal volume of 80 μM H_2O_2, resulting in a final volume of 25 μL. The reaction was quenched at various times between 0 and 15 s by the addition of 1 mL of FOX reagent.[50] The absorbance at 560 nm was determined using the Agilent spectrophotometer, and the amount of peroxide remaining in the solution was calculated by comparison with standard solutions of H_2O_2.

RESULTS AND DISCUSSION

***E. coli* BCP Is a Monomer in Solution Even at Concentrations as High as 200 μM.** Of the six described subfamilies of Prx proteins, only the proteins within the BCP/PrxQ class of Prxs are described as monomeric. Although this was originally thought to be characteristic of the subfamily as a whole, recent crystallographic analyses have demonstrated that some members of the BCP/PrxQ group are indeed dimeric.[17] In fact, the oligomeric state of *E. coli* BCP in solution over a range of concentrations has not been rigorously tested, although intersubunit disulfide bond formation was ruled out by SDS−polyacrylamide gel analysis and high-resolution mass spectrometry (MS).[24,26] We therefore used analytical ultracentrifugation analyses to determine the oligomeric state of reduced and oxidized BCP in solution at concentrations as high as 200 μM. As shown in Figure 1A, both redox forms of BCP exhibit sedimentation coefficients around 2 S; together with the diffusion coefficient measured from the same experiments, these data and the Svedberg equation yield shape-independent molecular masses of 19.4 and 22.2 kDa for reduced and oxidized BCP, respectively (given a theoretical mass for *E. coli* BCP of 17502.7 Da). No evidence of higher-order species was observed. Thus, in either redox state, *E. coli* BCP remains monomeric in solution even at very high concentrations.

As mentioned above, of the structural representatives of the BCP/PrxQ subfamily characterized by X-ray crystallography to date, four were monomeric, while two members crystallized as dimers (through the A-type interface commonly used to form PrxV and Tpx subfamily dimers). Unfortunately, no peer-reviewed publications have resulted from the dimeric structures of these *Aeropyrum pernix* (PDB entries 2cx3 and 2cx4) and *Sulfolobus tokadaii* BCP proteins (PDB entry 2ywn), so limited information is available. Nonetheless, an analysis of these structures as well as sequences of all BCP/PrxQ subfamily members (identified during a search of the January 2009 release

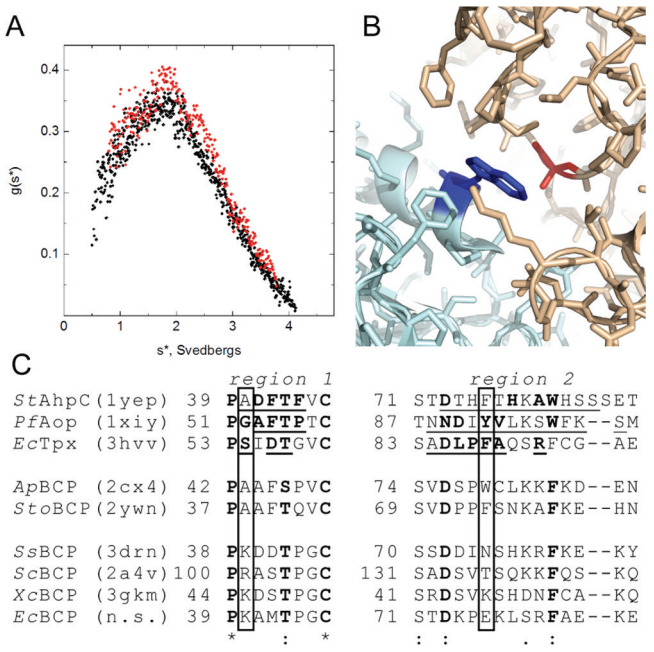

Figure 1. Monomeric nature of *E. coli* BCP, confirmed by sedimentation velocity studies, consistent with nonconserved residues within the region of the A-type interface. As shown in panel A, analytical ultracentrifugation studies of *E. coli* BCP at 42000 rpm, 20 °C, and neutral pH show no evidence of the formation of dimers or higher-order multimers using 50 μM reduced (red) and oxidized (black) wild-type BCP. SVEDBERG software was used to generate the $g^*(s)$ distributions shown in panel A and to fit the data to a single-species model, yielding molecular masses derived from extrapolated and corrected s and D values of 19.4 kDa for reduced and 22.2 kDa for oxidized BCP. Panel B depicts the A-type interface between dimers in *Aeropyrum pernix* BCP (PDB entry 2cx4), with one monomer colored light blue and the other tan. Upon comparison of monomeric BCPs (bottom of panel C) with the two dimeric BCPs (middle two lines) and members of three other A-type interface-containing Prx subfamilies (top part of panel C), it is notable that the dimeric proteins possess a conserved aromatic residue in region 2 (Trp79 in *A. pernix* BCP, blue residue in panel B) and a conserved small, mostly hydrophobic residue in region 1 (Ala43 in *A. pernix* BCP, red residue in panel B); these positions in *E. coli* BCP and three other monomeric BCPs instead have hydrophilic and mostly charged residues, consistent with their exposure to solvent in these monomers. Conserved residues within the given subfamilies (bold) and those within A interfaces (underlined) in the top three proteins were identified in a bioinformatics and structural analysis of subfamily members across all Prxs identified from a search of the January 2008 release of GenBank (January 2009 for BCP/PrxQ subfamily members).[6] Representative proteins shown are from *Salmonella typhimurium* (*St*), *Plasmodium falciparum* (*Pf*), *E. coli* (*Ec*), *A. pernix* (*Ap*), *S. tokadaii* (*Sto*), *Sulfolobus solfataricus* (*Ss*), *Saccharomyces cerevisiae* (*Sc*), and *Xanthomonas campestris* (*Xc*). n.s. indicates that there are no structural data available for *Ec*BCP.

of GenBank[6]) has revealed a location within the A-type interface of dimeric BCP proteins in which an aromatic residue from one monomer packs against a small, often hydrophobic residue (Figure 1B); the residues involved in this packing interaction are conserved across the three other Prx subfamilies that form A-type interfaces (Figure 1C). The presence of bulkier, charged residues in these positions may explain the lack of dimer formation in *E. coli* BCP and other monomeric subfamily members (Figure 1C).

E. coli BCP Exhibits Nonsaturable Interactions with Trx1 and Broad Specificity for Peroxide Substrates.

Previous assays conducted by Jeong et al.,[24] which used a single concentration of Trx1 (0.8 μM) and amounts of BCP that were equivalent to or in excess of the concentration of Trx1, yielded apparent V_{max} values for BCP with H_2O_2 of 7 μM peroxide substrate reduced min^{-1} (μM BCP)$^{-1}$. Our initial assays of *E. coli* BCP with Trx1 in excess yielded rates higher than those previously reported; furthermore, rates with Trx1 concentrations as high as 40 μM continued to increase, with no evidence of saturation (data not shown). A range of assays were therefore employed to better establish the kinetic attributes of this system.

As the BCP reaction can be monitored directly by the loss of Trx1 fluorescence as it becomes oxidized, we conducted a bisubstrate kinetic analysis of BCP with H_2O_2 and Trx1 using a stopped-flow spectrofluorometer to monitor turnover. Under these conditions, an increase in $V_{max,app}$ and $K_{m,app}$ for H_2O_2 was observed with increasing Trx1 concentrations as high as 80 μM, indicating an interaction between the reductant and BCP that is nonsaturable at physiologically reasonable concentrations (Figure 2A,B). Extrapolated values from global fits of all the

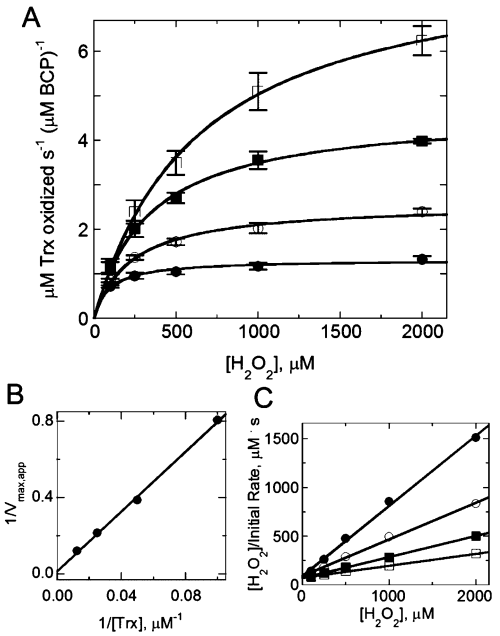

Figure 2. Steady state kinetic analyses of *E. coli* BCP with H_2O_2 and Trx1. Peroxidase activity was measured by mixing various concentrations of *E. coli* Trx1 (prereduced by DTT) and BCP (0.5 μM) in 50 mM potassium phosphate (pH 7.0) (with 0.5 mM EDTA) with various concentrations of H_2O_2 in a stopped-flow spectrophotometer at 25 °C. The decrease in Trx fluorescence due to oxidation was monitored and converted to the initial rate as described in Experimental Procedures. Fixed concentrations of Trx1 assayed over a range of H_2O_2 concentrations were 10 (●), 20 (○), 40 (■), and 80 μM (□). Data shown in panel A (±standard error) are averages of three independent replicates. Lines through the points show the direct fits to the Michaelis–Menten equation for each Trx1 concentration. (B) Secondary plot of $1/V_{max,app}$ vs 1/[Trx] from data shown in panel A and Table S1 of the Supporting Information. (C) Hanes–Woolf plot of $[H_2O_2]/v$ vs $[H_2O_2]$ from data shown in panel A and Table S1. Lines intersecting at the y-axis are consistent with a substituted (ping-pong) enzyme mechanism.

dx.doi.org/10.1021/bi200935d | *Biochemistry* 2011, 50, 8970–8981

Table 1. Steady State Kinetic Parameters of BCP Using 10 μM Trx1 or $Grx1_{F6W}$ and Varying Hydroperoxide Substrates Measured by Stopped-Flow Fluorescence Analysis

protein reductant, at 10 μM	ROOH[a]	$V_{max,app}$ [μM s^{-1} (μM BCP)$^{-1}$]	$K_{m,app}$ for ROOH (μM)	V_{max}/K_m (M^{-1} s^{-1})
Trx1	H_2O_2	1.24 ± 0.02	76.1 ± 3.9	1.6×10^4
	CHP	1.21 ± 0.02	99.5 ± 5.2	1.2×10^4
	*t*BHP	(1.6 ± 2.2)[b]	(6800 ± 11000)[b]	2.3×10^2
$Grx1_{F6W}$	H_2O_2	0.104 ± 0.006	14.6 ± 4.9	7.1×10^3
	CHP	0.128 ± 0.002	21.6 ± 1.3	5.9×10^3
	*t*BHP	0.124 ± 0.039	574 ± 294	2.2×10^2

[a]Abbreviations for hydroperoxide substrates are CHP for cumene hydroperoxide and *t*BHP for *tert*-butyl hydroperoxide. [b]Because of a very high apparent K_m, these values are poorly determined; data gathered included *t*BHP concentrations as high as 2 mM.

data for the K_m for Trx and for V_{max} are far outside the range of the data, at ~500 μM and 64 s^{-1}, respectively. Nonetheless, Hanes–Woolf treatment of the data is consistent with a ping-pong mechanism (Figure 2C). This lack of saturation with Trx1 demonstrates a major difference between BCP and many other Trx-dependent Prxs, including Tpx from *E. coli*; the latter protein interacts saturably with Trx1 during turnover with peroxide substrates (K_m for Trx1 of 25 μM).[5] Two other BCP/PrxQ subfamily members, from *Xylella fastidiosa* and poplar, were examined using similar kinetic approaches and also exhibited saturable interactions with both the reducing and oxidizing substrates (K_m values of 7 and 1.5 μM for their Trx reductants, respectively),[20,51] indicating that saturability by Trx1 is at least sometimes observed for members of the BCP/PrxQ subfamily.

Although the values for $V_{max,app}$ and $K_{m,app}$ for H_2O_2 changed with the concentration of Trx1 used, the $(V_{max}/K_m)_{app}$ for H_2O_2 remained constant at the various Trx1 concentrations used as expected for a ping-pong mechanism, giving an overall value of ~1.3×10^4 M^{-1} s^{-1} (Table S1 of the Supporting Information). This matches well with the value of V_{max}/K_m for H_2O_2 obtained as the reciprocal of the *y*-intercept in the Hanes–Woolf plot (1.2×10^4 M^{-1} s^{-1}), an alternative way to analyze steady state kinetic data (Figure 2C). This value is in the same range as the values of ~4×10^4 and ~8×10^3 M^{-1} s^{-1} obtained for the *X. fastidiosa* and poplar PrxQ proteins, respectively,[20,51] and rather higher than the original estimate of 2.45×10^3 M^{-1} s^{-1} for *E. coli* BCP reported by Jeong et al.[24] This catalytic efficiency is somewhat modest when compared with k_{cat}/K_m values obtained for Trx-dependent Prxs from other subfamilies, which typically exhibit values for their best substrates as high as 10^7 or 10^8 M^{-1} s^{-1}.[15,52] Interestingly, *E. coli* Tpx, which reduces organic hydroperoxides much more efficiently, has a very high K_m for H_2O_2 (~1.7 mM) and consequently a very similar k_{cat}/K_m value for H_2O_2 (4.4×10^4 M^{-1} s^{-1}) compared with that for BCP.[5]

To directly compare *E. coli* BCP activity with different peroxide substrates, a physiologically reasonable Trx1 concentration of 10 μM was chosen for these analyses (based on cellular concentrations of ~10–30 μM[53,54]). Using Trx1, the apparent K_m value for H_2O_2 is ~80 μM and similar to the value obtained for cumene hydroperoxide; the $V_{max,app}$ values for these two substrates are also very similar (Table 1). A related hydroperoxide substrate lacking the aromatic ring, but with a methyl group in its place, *tert*-butyl hydroperoxide, is a very poor substrate under these conditions (Table 1 and Figure S1 of the Supporting Information). The similarity between H_2O_2 and cumene hydroperoxide as substrates and the demonstration that *tert*-butyl hydroperoxide is a worse substrate for *E. coli* BCP are consistent with the trend seen with the kinetically characterized PrxQ enzymes from *X. fastidiosa* and poplar, although the differences between the two organic hydroperoxides were not so striking in those cases.[20,51]

Multiple Trx and Grx Proteins Are Functionally Relevant Reductants of *E. coli* BCP. Although most Prxs that use Trx substrates for reductive recycling do not show significant activity with Grx proteins (smaller, CXXC-containing Trx fold proteins present in many organisms), some degree of overlapping substrate specificity between these reductants and specific Prxs has been observed, e.g., in a plant PrxII subgroup member from poplar phloem (in the PrxV subfamily),[55,56] in mitochondrial Prx1p from *Saccharomyces cerevisiae* (a human PrxVI-like protein),[57] in human PrxIII,[58] and in members of the BCP/PrxQ subfamily.[29,51] Other cases in which a Grx is or may be the physiological reductant of a Prx include the bacterial Prx–Grx hybrid proteins within the Prx5 subfamily[59,60] and an unusual system from *Clostridium pasteurianum* in which the Prx1/AhpC protein (denoted Cp20) is recycled by Trx reductase (Cp34)- and Grx (Cp9)-related proteins expressed from the same operon.[61] There is also a second Trx protein in *E. coli*, Trx2, which has properties distinct from those of Trx1[62] and has not previously been investigated as a potential BCP reductant. To quantitatively evaluate the specific contributions of Trx- and Grx-linked pathways to recycling of *E. coli* BCP during turnover with peroxides, we expressed and purified both Trx proteins (Trx1 and Trx2), as well as the two small, CXXC-containing Grx proteins from *E. coli* (Grx1 and Grx3). The two Grx proteins that were not evaluated were Grx2, which is much larger and more closely related to the glutathione *S*-transferases,[63,64] and Grx4, which is a "monothiol" Grx with CXXS at the active site instead of CXXC.[65] Multicomponent, NADPH-dependent assays were used, keeping conditions as nearly identical as possible. These assay mixtures all contained NADPH, a small amount of BCP (0.5 μM), 1 mM cumene hydroperoxide, and the reductant being tested (10 μM); assays also included either TrxR (0.1 μM) or glutathione (1 mM) and glutathione reductase (1 unit/mL), as the recycling systems for Trx and Grx, respectively. AhpF, the physiological reductant of AhpC, was also tested in similar assays but exhibited no detectable activity with BCP (not shown). Under these conditions, the most active reductant (Trx1) differed less than 6-fold from the least active (Grx3) in terms of the rate of turnover (Figure 3A). To gain insight into how much each reductant might be expected to contribute to the reductive recycling of *E. coli* BCP in vivo, we combined previously published data regarding the abundance of each reductant during exponential or stationary phases of growth[66] with these rates to estimate their relative contributions in *E. coli* (Figure 3B). Thus, because of its abundance, Grx3 is likely to contribute more to BCP reduction than Grx1 even though it exhibits a more moderate rate of

dx.doi.org/10.1021/bi200935d | *Biochemistry* 2011, 50, 8970–8981

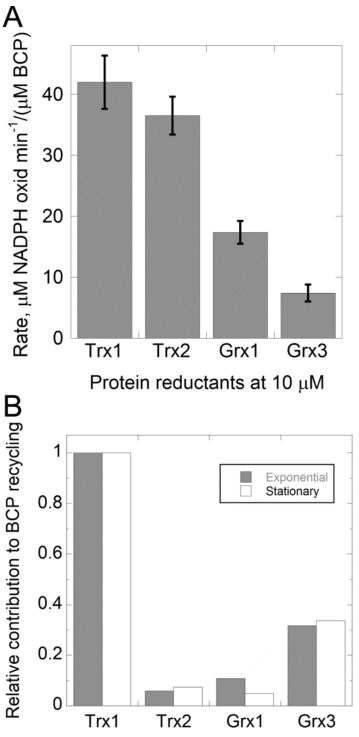

Figure 3. Reductants of *E. coli* BCP. Thioredoxin (Trx) and glutaredoxin (Grx) proteins from *E. coli* were assayed with BCP in a common buffer that differed only in the appropriate regeneration system for each (Trx reductase or glutathione reductase and glutathione, respectively). Assays were conducted in 50 mM phosphate buffer (pH 7.0) with 1 mM EDTA, 150 μM NADPH, 0.5 μM BCP, 1 mM cumene hydroperoxide, and 10 μM Trx1, Trx2, Grx1, or Grx3. For Trx-linked assays, 0.3 μM *E. coli* Trx reductase was also added; the Grx-linked assays were supplemented instead with 1 mM reduced glutathione and 1 unit/mL glutathione reductase. Activity was monitored spectrophotometrically at 340 nm, and initial rates were used to calculate the amount of NADPH oxidized per minute normalized to the amount of BCP added. Shown are averages from at least three experiments ± the standard error. Also tested was a reductant system including NADH and AhpF in addition to the BCP and peroxide, but no activity was observed; thus, this result is not included in the plot. In panel B, abundance in nanograms per milliliter for each protein[66] was multiplied by the rate reported in panel A, and the product was normalized to 1.0 for Trx1.

turnover with BCP (Figure 3A,B). This treatment of data does not take into account, however, the fact that under high-oxidative stress conditions, when OxyR is activated and transcriptionally upregulating *trxC* (Trx2) expression, the level of Trx2 can actually rise to a point where it becomes more abundant than Trx1,[37] thus suggesting that all four of these reductants may contribute meaningfully to the cellular reducing power that sustains BCP peroxidase activity.

As previously established in studies of AhpC and other Prxs, assays that utilize only one concentration of reductant and/or one concentration of peroxide may give somewhat deceptive results.[15] Therefore, we focused our efforts on conducting a full kinetic analysis with *E. coli* Grx1 varying both reductant and peroxide, as described above for Trx1. Initial experiments established, however, that the low fluorescence emission of Grx1, in combination with a similar fluorescence signal being contributed by BCP, even at low concentrations, obviated the use of an approach similar to that used with Trx1 (Figure 2).[36] To circumvent this problem, we engineered a new fluorescent tryptophan into Grx1 in a position near the active site CXXC where a bulky residue was already present, creating the F6W mutant of this protein. This mutant is highly fluorescent, and the fluorescence changes substantially with redox state.[36] As verified by the commonly used HED assays for Grx proteins, the mutant $Grx1_{F6W}$ exhibited activity equivalent to that of the wild-type protein using this small molecule substrate.[36] In an extension of these studies, the same multiprotein assays used above to compare the various Trx and Grx reductants (Figure 3) established that the mutation caused little, if any, change in activity in a full peroxidase assay with BCP and peroxide [15.8 ± 1.5 μM s^{-1} (μM BCP)$^{-1}$ for the F6W mutant compared with 17.4 ± 1.9 μM s^{-1} (μM BCP)$^{-1}$ for wild-type Grx1]. Using the full bisubstrate analysis of BCP with various concentrations of $Grx1_{F6W}$ and peroxides, we found that the catalytic efficiency (V_{max}/K_m) of BCP with H_2O_2 is within ~2-fold of this value with Trx1 (7.1×10^3 M^{-1} s^{-1}), and the relative reactivities with the different hydroperoxide substrates using Grx1 mirror those with Trx1 (Table 1 and Figure S1 of the Supporting Information). Nonetheless, the $V_{max,app}$ and $K_{m,app}$ values for peroxides are both lower with Grx1 than with Trx1; this may reflect greater limitation in the reductive recycling of BCP by Grx1 than by Trx1, yielding a $K_{m,app}$ value for H_2O_2 "artificially" lower than what would be observed with a better reductant or poorer peroxide substrate (supported by data in Table 1).

Previous studies have demonstrated that the *E. coli* Prx with greatest activity on organic hydroperoxides, Tpx, is functional only with Trx1 and not Trx2 or Grx1.[5] To establish whether broad reductant specificity is unique (among the *E. coli* Prxs) to BCP, we also investigated the ability of *Salmonella typhimurium* AhpC (closely related to the *E. coli* enzyme) to function with Trx1 and Grx1 as alternatives to its native reductant, AhpF. Although turnover with H_2O_2 can be observed with AhpC in the presence of *E. coli* Trx1, the interaction between these two proteins to support catalysis is nonsaturable using Trx1 concentrations as high as 30 μM. If a single concentration of 10 μM is chosen for Trx1 and the S128W mutant of C-terminally truncated AhpF used in stopped-flow assays with AhpC,[46] the apparent V_{max} with H_2O_2 is much lower with Trx1, at ~1.7% of the value with the AhpF derivative. The rate of reaction of AhpC with H_2O_2 in the presence of $Grx1_{F6W}$ is even lower.

The Midpoint Reduction Potential of BCP Is Very High, Consistent with the High Reactivity of This Protein toward Multiple Reductants. The midpoint reduction (redox) potentials of the two Trx and two Grx proteins studied above vary widely (−198 mV for Grx3, −221 mV for Zn-replete Trx2, −233 mV for Grx1, and −284 or −270 mV for Trx1),[62,67] but all act as rather efficient reductants of BCP during turnover with peroxides. However, the only known redox potential for members of this Prx subfamily is for the poplar PrxQ protein, at −325 mV,[51] a very low redox potential that would hinder electron transfer from all but the most reducing of the Trx/Grx proteins. In the plant chloroplast, this redox potential is well suited to the role of Prxs in protection against oxidants where the Prx must be compatible with the unique, light-driven redox cycles of this photosynthetic organelle.[23,68] As BCP functions, instead, in the cytoplasm of *E. coli*, it was important to determine the redox potential for *E. coli* BCP to improve our understanding of its functional attributes contributing to catalysis.

To determine the redox potential of BCP, we modified an approach used successfully in our hands to determine the redox

potentials of two bacterial AhpC proteins[15,69] in which a protein of unknown potential is equilibrated with another of known potential and the amount of oxidized and reduced species in the equilibrated mixtures can be used to calculate the redox potential of the unknown protein using a derivation of the Nernst equation.[67] When BCP was equilibrated with Grx1, an approach that worked well for the two AhpC proteins, Grx1 was fully oxidized and BCP was fully reduced, indicating that the redox potential of the BCP was more than 50 mV higher than that of the test protein (data not shown). We then expressed and purified *E. coli* DsbA for the equilibration as it has a much higher redox potential (see Experimental Procedures). Briefly, reduced BCP and oxidized DsbA at pH 7 and room temperature were mixed, equilibrated for 6 h (an equilibration time that was verified to be sufficient in preliminary experiments), quenched by addition of NEM followed by acid, and then resolved by HPLC to quantify the respective redox forms of the two proteins (Figure 4, red). In

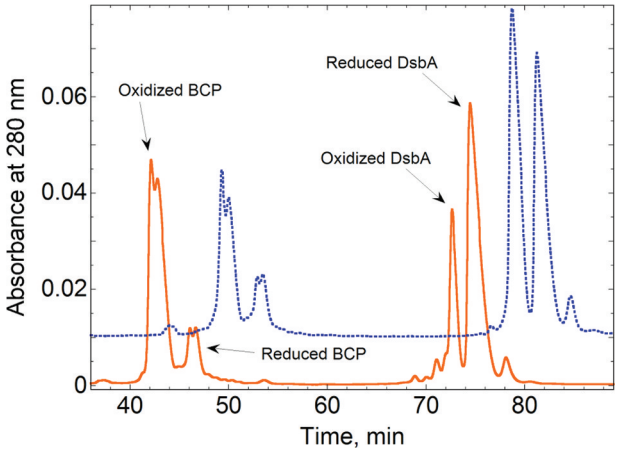

Figure 4. HPLC profile of the separation of equilibrated reduced and oxidized forms of *E. coli* BCP and DsbA to determine redox potential. Reduced and oxidized BCP and DsbA (each at 50 μM) were allowed to equilibrate at room temperature in 100 mM potassium phosphate (pH 7.0) with 1 mM EDTA. The protein mixtures were quenched with *N*-ethylmaleimide and phosphoric acid and immediately separated by HPLC as described in Experimental Procedures. Shown are the chromatograms from mixing of reduced BCP with oxidized DsbA (red) and, displaced by 7 min and 0.01 absorbance unit for ease of viewing, reduced DsbA mixed with oxidized BCP (blue).

three independent replicates, a value for the redox potential of BCP of −152.6 ± 1.2 mV was obtained. Similarly, three replicates of the reverse experiment (reduced DsbA mixed with oxidized BCP) yielded a redox potential of −139.2 ± 2.2 mV (Figure 4, blue). Averaging all values yielded a final redox potential value of −145.9 ± 3.2 mV for *E. coli* BCP. This value is the highest determined redox potential for a Prx to date and strikingly different from that of the poplar PrxQ in the same subfamily, which is the lowest reported value among all Prxs studied so far.[23,51,70] Like the values previously obtained for *Treponema pallidum* AhpC and *S. typhimurium* AhpC (−192 ± 2 and −178 ± 0.4 mV, respectively),[15,69] this is a relatively high redox potential compared with those of many other redox disulfide-containing proteins and is consistent with the reduction of BCP being thermodynamically favorable with a wide range of reductants.

While a favorable thermodynamic driving force is irrelevant if no kinetically competent pathway exists for the exchange of electrons between two proteins, the redox potentials are very important in that they govern the ratio of the reduced and oxidized forms of each of the two proteins at equilibrium. Thus, it is critical to establish the actual kinetic competence of electron transfer when identifying relevant reductants of a given oxidized protein, as we have done in the kinetic experiments described above. Our data indicate that *E. coli* BCP will be nearly completely reduced when equilibrated with equimolar amounts of either fully reduced Trx or fully reduced Grx (with reduced BCP fraction of >99% or >96% for Trx1 and Grx1, respectively). It should also be noted that an electron donor may in fact have a higher redox potential than its protein partner as long as they are reasonably close in potential (within less than ~100 mV), as is the case with poplar PrxQ and its physiological reductant, Trx (with redox potentials of −325 and approximately −290 mV, respectively). In such a case, fully reduced Trx mixed with fully oxidized PrxQ would reach an equilibrium state of 20% reduced PrxQ and 80% reduced Trx (in the absence of further reduction of Trx or oxidation of PrxQ). At equilibrium, the forward and back reactions both occur with the same overall flux, leading to no net change in the populations of the reduced and oxidized proteins. However, electron transfer in living systems is a very dynamic process, and the re-reduction of Trx ensures that the forward reaction continues with a greater flux than the back reaction, allowing a significant complement of reduced PrxQ to be maintained for peroxide reduction in spite of their "inverted" redox potentials. In contrast, the redox potential is much higher for Grx (−230 mV) than for PrxQ (−325 mV);[51] thus, even if a facile kinetic pathway exists, only 2.4% of PrxQ would be reduced before equilibrium was reached in the absence of further electron-transferring partners. These studies establish that BCP reduction by Trx and Grx is favored both thermodynamically and kinetically.

The pK_a of the Peroxidatic Cysteine of *E. coli* BCP Is <6, Similar to Those of *X. fastidiosa* PrxQ, *S. typhimurium* AhpC, and Other Prxs. To react efficiently with peroxides, the C_p in Prxs needs to be deprotonated; therefore, Prx activity is supported by the lowered pK_a of the C_p. Before embarking on pK_a analyses of BCP, we assessed the stability of this protein across a range of pH values to avoid conducting uninformative experiments. Both fluorescence measurements for monitoring unfolding and experiments for evaluating activity retention after low- or high-pH treatment indicated that BCP is resistant to irreversible denaturation across the full pH range from 3 to 9. This result differs from that with AhpC, which showed instability in buffers below pH ~4.2.[32]

Attempts to measure the pH dependence of BCP activity were made through assessment of the competition between BCP and horseradish peroxidase (HRP) for hydrogen peroxide,[20,32,71] but the apparently slow reaction of BCP under these conditions did not allow us to use this approach as it competed very poorly with HRP. We therefore turned to an approach whereby absorbance at 240 nm is used to monitor the protonation state of cysteine residues in proteins.[32,72−74] Given the stability results described above, the ε_{240} was determined for both oxidized and reduced wild-type BCP over the pH range between 3 and 9. While the oxidized protein did not exhibit a significant pH-dependent change in ε_{240}, the reduced protein exhibited a single apparent pK_a value of 5.76 ± 0.08

dx.doi.org/10.1021/bi200935d | *Biochemistry* 2011, 50, 8970−8981

(Figure 5A). Although reduced, wild-type BCP possesses three cysteinyl residues, data obtained are consistent with titration of

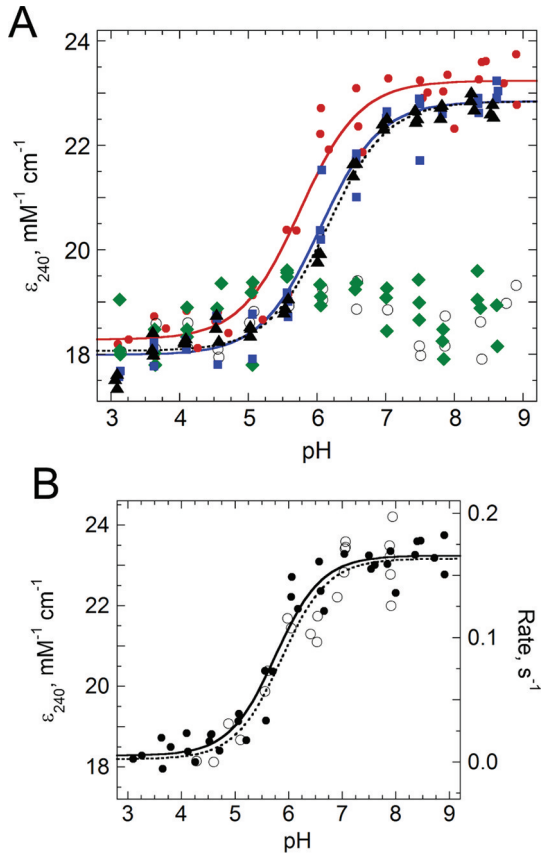

Figure 5. Effects of pH on absorbance at 240 nm (A and B) and activity measured by the FOX assay (B) for BCP proteins. To generate data shown in both panels, the A_{240} and A_{280} values for reduced BCP (25 μM) were measured over a range of pH values and converted to ε_{240} as described in Experimental Procedures. Assuming the change in absorbance reflects a simple thiolate:thiol equilibrium, the pK_a values were calculated from the plot of ε_{240} vs pH by a direct fit to eq 3. Values shown are for wild-type (red circles), C50S (blue squares), and C50,99S (black triangles) BCP, along with the respective pK_a fit curves (solid red, solid blue, and dotted black lines, respectively). Data for C45S (green triangles) and oxidized wild-type BCP (○) are also shown. In panel B, peroxide reduction rates (right axis) were assessed using the FOX assay to measure peroxide levels after rapid mixing with BCP (over a time course of 1−15 s), monitoring the decrease in absorbance at 560 nm after addition of the reagent (open circles and dotted line for the fit to eq 3). These data are overlaid with the data from panel A with reduced, wild-type BCP (filled circles and solid line) to illustrate the agreement between these independently derived apparent pK_a values.

only one thiol group, or multiple thiol groups with indistinguishable pK_a values around 5.8. As our interest is very specifically in the pK_a value of the peroxidatic Cys that lies within the active site, mutants were prepared via removal of one (C_r, Cys50) or both (Cys50 and Cys99) of the other Cys residues in the protein by replacement with Ser. In each of these mutants, the pH dependence of ε_{240} was shifted slightly to the right, yielding values of 6.05 ± 0.07 and 6.16 ± 0.05 for C50S and C50,99S, respectively. In contrast, the mutant lacking C_p (C45S) is much more reminiscent of the oxidized protein and seems to lack any clear increase in absorbance as the pH increases (Figure 5A). The magnitude of the absorbance change was very similar for both C_r mutants (C50S and C50,99S) and the wild-type protein, suggesting that each of these curves reflects primarily, or solely, the C_p thiol/thiolate status. The upward shift of ~0.3−0.4 pH unit for both mutants that lack the C_r likely reflects the moderate influence this residue has on the C_p pK_a, presumably through structural and electrostatic perturbations near the active site imparted by this mutation.

To provide an independent measure of the pK_a of the C_p thiol group, we evaluated the rate of reaction of BCP with H_2O_2 using rapid manual mixing of enzyme (20 μM) and substrate (40 μM), quenching of the reaction with the FOX reagent, and subsequent spectrophotometric analysis to detect the disappearance of peroxide at time points from 1 to 15 s. The amount of peroxide consumed following addition of reduced BCP was stoichiometric, verifying the complete reduction of the protein prior to the assay. Under these conditions, a first-order rate of around 0.17 s^{-1} was obtained at pH 7 that, when divided by the concentration of BCP used, yields a second-order rate constant of 9 × 10^3 M^{-1} s^{-1}, matching well with the V_{max}/K_m value for peroxide established in the steady state assays with Trx1. As shown in Figure 5B, titration of the BCP peroxide reactivity gave a remarkably similar pK_a value of 5.87 ± 0.16, strongly supporting the interpretation that the pK_a value of ~5.8 observed for the reduced, wild-type enzyme by monitoring absorbance changes at 240 nm predominantly reflects titration of the C_p thiol group. This pK_a value for BCP is quite similar to those of other Prxs studied previously,[52] including *X. fastidiosa* PrxQ (6.2) and *S. typhimurium* AhpC (5.9).[20,32]

CONCLUSIONS

With these studies, we show that *E. coli* BCP exhibits similar levels of activity with a variety of both peroxides and reducing partners. Notably, *E. coli* BCP is one of the relatively few Prxs across the diverse family that can be reduced by glutaredoxins.[29,55,57,60,61] BCP can take advantage of the availability of multiple forms of both Trx and Grx, in part because of its very high redox potential, and exhibits activity with both small and large hydroperoxide substrates, making it a potentially very important back-up system in cells with compromised redox pathways. Even under highly oxidizing cellular conditions, BCP would be able to maintain its peroxidase activity through interaction with virtually any available reductant and catalyze the reduction of a variety of peroxides, thus potentially serving as a defense enzyme of last resort. This functional flexibility may exist at the cost of a notably slower reactivity with peroxide (with a k_{cat}/K_m for peroxide of ~10^4 M^{-1} s^{-1}) as compared to the two other Prxs present in *E. coli* (AhpC and Tpx). These two Prxs exhibit much higher activities with the preferred substrates but are also much more specific in the peroxide and reducing substrates used.[5,7,15]

Interestingly, the second-order rate constant of 9 × 10^3 M^{-1} s^{-1} obtained by monitoring the disappearance of peroxide in the presence of BCP indicates that the steady state value for k_{cat}/K_m for peroxide does reflect a slow rate of reaction of the reduced enzyme with H_2O_2 (Figure 5B). This is in contrast to the findings with *X. fastidiosa* PrxQ, for which the first step of peroxide reaction is actually much faster (~10^7 M^{-1} s^{-1}) than its overall k_{cat}/K_m for H_2O_2 (~10^4 M^{-1} s^{-1}).[20] Both *E. coli* BCP and *X. fastidiosa* PrxQ do, however, stabilize the thiolate form of the peroxidatic Cys in the active site to approximately the same degree (pK_a values of ~5.8 and ~6.2, respectively).[20]

dx.doi.org/10.1021/bi200935d | *Biochemistry* 2011, 50, 8970−8981

Differences between these enzymes also extend to the location of their resolving cysteines. While the resolving cysteine in *E. coli* BCP is found in the same helix, α2, as the C_p, the C_r in *X. fastidiosa* PrxQ is found in helix α3, as is commonly the case in Tpx subfamily members, but also observed in ~7% of the BCP/PrxQ subfamily members.[6] Taken together, these differences support the assignment of *E. coli* BCP and *X. fastidiosa* PrxQ to two separate subgroups within the BCP/PrxQ subfamily.[75]

Although the BCP/PrxQ subfamily members can confidently be grouped together on the basis of sequence analyses that emphasize features near the active site,[6,22,76] they are a very diverse set of proteins spread across much of the phylogenetic tree. With these data, we note that *E. coli* BCP has the highest redox potential (−146 mV at pH 7) and poplar PrxQ the lowest redox potential (−325 mV at pH 7) among all Prxs studied so far, indicating quite different structural attributes for the disulfide bonds in these proteins. It is now clear that some BCP/PrxQ proteins are monomeric, while others are dimeric. Even the second-order reaction rate with H_2O_2 is now known to vary by as much as 3 orders of magnitude across the subfamily.[20] It is perhaps this very "adaptability" that has led to the persistence of this subfamily through much of evolution, adapting to fill a need in the various organisms that express it.[24,25,77,78]

■ ASSOCIATED CONTENT

Supporting Information

One additional table (Table S1) and figure (Figure S1). This material is available free of charge via the Internet at http://pubs.acs.org.

■ AUTHOR INFORMATION

Corresponding Author

*Telephone: (336) 716-6711. Fax: (336) 777-3242. E-mail: lbpoole@wakehealth.edu.

Funding

This study was supported by a grant from the National Institutes of Health to L.B.P. (RO1 GM050389), including a Research Supplement to Promote Diversity in Health-Related Research for S.A.R.

■ ACKNOWLEDGMENTS

We thank Mark Morris and Mark Lively of the Wake Forest University Bioanalytical Laboratory (supported in part by the Comprehensive Cancer Center of Wake Forest University and National Institutes of Health Grant P30 CA012197) for assistance in the analysis of the redox potential. Laura Cookman assisted with PCR and subcloning of the *bcp* gene from *E. coli*. The expression system for Trx1 was a kind gift from Dr. Charles Williams, Jr. We also thank Dr. Jon Beckwith and colleagues for providing the expression plasmids for the Trx2, Grx3, and DsbA proteins from *E. coli*.

■ ABBREVIATIONS

Prx, peroxiredoxin; BCP, bacterioferritin comigratory protein; C_p, peroxidatic cysteine (C45 of *E. coli* BCP); C_r, resolving cysteine (C50 of *E. coli* BCP); Tpx, thiol peroxidase; Trx, thioredoxin; Grx, glutaredoxin; DTNB, 5,5′-dithiobis(2-nitrobenzoic acid); SDS, sodium dodecyl sulfate; DTT, 1,4-dithiothreitol; GuHCl, guanidine hydrochloride; DTPA, diethylenetriaminepentaacetic acid; EDTA, ethylenediaminetetraacetic acid; MS, mass spectrometry; IPTG, isopropyl 1-thio-β-D-galactopyranoside; $Grx1_{F6W}$, F6W mutant of Grx1; PDB, Protein Data Bank.

■ REFERENCES

(1) Imlay, J. A. (2008) Cellular defenses against superoxide and hydrogen peroxide. *Annu. Rev. Biochem. 77*, 755−776.

(2) Eschenbach, D. A., Davick, P. R., Williams, B. L., Klebanoff, S. J., Young-Smith, K., Critchlow, C. M., and Holmes, K. K. (1989) Prevalence of hydrogen peroxide-producing *Lactobacillus* species in normal women and women with bacterial vaginosis. *J. Clin. Microbiol. 27*, 251−256.

(3) Miller, R. A., and Britigan, B. E. (1997) Role of oxidants in microbial pathophysiology. *Clin. Microbiol. Rev. 10*, 1−18.

(4) Ryan, C. S., and Kleinberg, I. (1995) Bacteria in human mouths involved in the production and utilization of hydrogen peroxide. *Arch. Oral Biol. 40*, 753−763.

(5) Baker, L. M., and Poole, L. B. (2003) Catalytic mechanism of thiol peroxidase from *Escherichia coli*. Sulfenic acid formation and overoxidation of essential CYS61. *J. Biol. Chem. 278*, 9203−9211.

(6) Nelson, K. J., Knutson, S. T., Soito, L., Klomsiri, C., Poole, L. B., and Fetrow, J. S. (2011) Analysis of the peroxiredoxin family: Using active-site structure and sequence information for global classification and residue analysis. *Proteins 79*, 947−964.

(7) Poole, L. B. (2005) Bacterial defenses against oxidants: Mechanistic features of cysteine-based peroxidases and their flavoprotein reductases. *Arch. Biochem. Biophys. 433*, 240−254.

(8) Poole, L. B., Reynolds, C. M., Wood, Z. A., Karplus, P. A., Ellis, H. R., and Li Calzi, M. (2000) AhpF and other NADH:peroxiredoxin oxidoreductases, homologues of low Mr thioredoxin reductase. *Eur. J. Biochem. 267*, 6126−6133.

(9) Jönsson, T. J., Ellis, H. R., and Poole, L. B. (2007) Cysteine reactivity and thiol-disulfide interchange pathways in AhpF and AhpC of the bacterial alkyl hydroperoxide reductase system. *Biochemistry 46*, 5709−5721.

(10) Neumann, C. A., Krause, D. S., Carman, C. V., Das, S., Dubey, D. P., Abraham, J. L., Bronson, R. T., Fujiwara, Y., Orkin, S. H., and Van Etten, R. A. (2003) Essential role for the peroxiredoxin Prdx1 in erythrocyte antioxidant defence and tumour suppression. *Nature 424*, 561−565.

(11) Winterbourn, C. C. (2008) Reconciling the chemistry and biology of reactive oxygen species. *Nat. Chem. Biol. 4*, 278−286.

(12) Wood, Z. A., Poole, L. B., and Karplus, P. A. (2003) Peroxiredoxin evolution and the regulation of hydrogen peroxide signaling. *Science 300*, 650−653.

(13) Zhang, B., Wang, Y., and Su, Y. (2009) Peroxiredoxins, a novel target in cancer radiotherapy. *Cancer Lett. 286*, 154−160.

(14) Woolston, C. M., Storr, S. J., Ellis, I. O., Morgan, D. A., and Martin, S. G. (2011) Expression of thioredoxin system and related peroxiredoxin proteins is associated with clinical outcome in radiotherapy treated early stage breast cancer. *Radiother. Oncol. 100*, 308−313.

(15) Parsonage, D., Karplus, P. A., and Poole, L. B. (2008) Substrate specificity and redox potential of AhpC, a bacterial peroxiredoxin. *Proc. Natl. Acad. Sci. U.S.A. 105*, 8209−8214.

(16) Hall, A., Karplus, P. A., and Poole, L. B. (2009) Typical 2-Cys peroxiredoxins: Structures, mechanisms and functions. *FEBS J. 276*, 2469−2477.

(17) Hall, A., Nelson, K., Poole, L., and Karplus, P. A. (2011) Structure-based insights into the catalytic power and conformational dexterity of peroxiredoxins. *Antioxid. Redox Signaling 15*, 795−815.

(18) Wood, Z. A., Poole, L. B., Hantgan, R. R., and Karplus, P. A. (2002) Dimers to doughnuts: Redox-sensitive oligomerization of 2-cysteine peroxiredoxins. *Biochemistry 41*, 5493−5504.

(19) Poole, L. B., Godzik, A., Nayeem, A., and Schmitt, J. D. (2000) AhpF can be dissected into two functional units: Tandem repeats of two thioredoxin-like folds in the N-terminus mediate electron transfer from the thioredoxin reductase-like C-terminus to AhpC. *Biochemistry 39*, 6602−6615.

(20) Horta, B. B., de Oliveira, M. A., Discola, K. F., Cussiol, J. R., and Netto, L. E. (2010) Structural and biochemical characterization of peroxiredoxin Qbeta from *Xylella fastidiosa*: Catalytic mechanism and high reactivity. *J. Biol. Chem. 285*, 16051−16065.
(21) Rouhier, N., and Jacquot, J. P. (2005) The plant multigenic family of thiol peroxidases. *Free Radical Biol. Med. 38*, 1413−1421.
(22) Copley, S. D., Novak, W. R., and Babbitt, P. C. (2004) Divergence of function in the thioredoxin fold suprafamily: Evidence for evolution of peroxiredoxins from a thioredoxin-like ancestor. *Biochemistry 43*, 13981−13995.
(23) Dietz, K. J. (2011) Peroxiredoxins in plants and cyanobacteria. *Antioxid. Redox Signaling 15*, 1129−1159.
(24) Jeong, W., Cha, M. K., and Kim, I. H. (2000) Thioredoxin-dependent hydroperoxide peroxidase activity of bacterioferritin comigratory protein (BCP) as a new member of the thiol-specific antioxidant protein (TSA)/alkyl hydroperoxide peroxidase C (AhpC) family. *J. Biol. Chem. 275*, 2924−2930.
(25) Wang, G., Olczak, A. A., Walton, J. P., and Maier, R. J. (2005) Contribution of the *Helicobacter pylori* thiol peroxidase bacterioferritin comigratory protein to oxidative stress resistance and host colonization. *Infect. Immun. 73*, 378−384.
(26) Clarke, D. J., Mackay, C. L., Campopiano, D. J., Langridge-Smith, P., and Brown, A. R. (2009) Interrogating the molecular details of the peroxiredoxin activity of the *Escherichia coli* bacterioferritin comigratory protein using high-resolution mass spectrometry. *Biochemistry 48*, 3904−3914.
(27) D'Ambrosio, K., Limauro, D., Pedone, E., Galdi, I., Pedone, C., Bartolucci, S., and De Simone, G. (2009) Insights into the catalytic mechanism of the Bcp family: Functional and structural analysis of Bcp1 from *Sulfolobus solfataricus*. *Proteins 76*, 995−1006.
(28) Liao, S. J., Yang, C. Y., Chin, K. H., Wang, A. H., and Chou, S. H. (2009) Insights into the alkyl peroxide reduction pathway of *Xanthomonas campestris* bacterioferritin comigratory protein from the trapped intermediate-ligand complex structures. *J. Mol. Biol. 390*, 951−966.
(29) Clarke, D. J., Ortega, X. P., Mackay, C. L., Valvano, M. A., Govan, J. R., Campopiano, D. J., Langridge-Smith, P., and Brown, A. R. (2010) Subdivision of the bacterioferritin comigratory protein family of bacterial peroxiredoxins based on catalytic activity. *Biochemistry 49*, 1319−1330.
(30) Storz, G., Jacobson, F. S., Tartaglia, L. A., Morgan, R. W., Silveira, L. A., and Ames, B. N. (1989) An alkyl hydroperoxide reductase induced by oxidative stress in *Salmonella typhimurium* and *Escherichia coli*: Genetic characterization and cloning of *ahp*. *J. Bacteriol. 171*, 2049−2055.
(31) Baba, T., Ara, T., Hasegawa, M., Takai, Y., Okumura, Y., Baba, M., Datsenko, K. A., Tomita, M., Wanner, B. L., and Mori, H. (2006) Construction of *Escherichia coli* K-12 in-frame, single-gene knockout mutants: The Keio collection. *Mol. Syst. Biol. 2*, 2006−0008.
(32) Nelson, K. J., Parsonage, D., Hall, A., Karplus, P. A., and Poole, L. B. (2008) Cysteine pK_a values for the bacterial peroxiredoxin AhpC. *Biochemistry 47*, 12860−12868.
(33) Veine, D. M., Mulrooney, S. B., Wang, P. F., and Williams, C. H. Jr. (1998) Formation and properties of mixed disulfides between thioredoxin reductase from *Escherichia coli* and thioredoxin: Evidence that cysteine-138 functions to initiate dithiol-disulfide interchange and to accept the reducing equivalent from reduced flavin. *Protein Sci. 7*, 1441−1450.
(34) Lennon, B. W., and Williams, C. H. Jr. (1995) Effect of pyridine nucleotide on the oxidative half-reaction of *Escherichia coli* thioredoxin reductase. *Biochemistry 34*, 3670−3677.
(35) Yamamoto, Y., Ritz, D., Planson, A. G., Jonsson, T. J., Faulkner, M. J., Boyd, D., Beckwith, J., and Poole, L. B. (2008) Mutant AhpC peroxiredoxins suppress thiol-disulfide redox deficiencies and acquire deglutathionylating activity. *Mol. Cell 29*, 36−45.
(36) Parsonage, D., Reeves, S. A., Karplus, P. A., and Poole, L. B. (2010) Engineering of fluorescent reporters into redox domains to monitor electron transfers. *Methods Enzymol. 474*, 1−21.
(37) Ritz, D., Patel, H., Doan, B., Zheng, M., Aslund, F., Storz, G., and Beckwith, J. (2000) Thioredoxin 2 is involved in the oxidative stress response in *Escherichia coli*. *J. Biol. Chem. 275*, 2505−2512.
(38) Ortenberg, R., Gon, S., Porat, A., and Beckwith, J. (2004) Interactions of glutaredoxins, ribonucleotide reductase, and components of the DNA replication system of *Escherichia coli*. *Proc. Natl. Acad. Sci. U.S.A. 101*, 7439−7444.
(39) Nordstrand, K., Aslund, F., Meunier, S., Holmgren, A., Otting, G., and Berndt, K. D. (1999) Direct NMR observation of the Cys-14 thiol proton of reduced *Escherichia coli* glutaredoxin-3 supports the presence of an active site thiol-thiolate hydrogen bond. *FEBS Lett. 449*, 196−200.
(40) Åslund, F., Ehn, B., Miranda-Vizuete, A., Pueyo, C., and Holmgren, A. (1994) Two additional glutaredoxins exist in *Escherichia coli*: Glutaredoxin 3 is a hydrogen donor for ribonucleotide reductase in a thioredoxin/glutaredoxin 1 double mutant. *Proc. Natl. Acad. Sci. U.S.A. 91*, 9813−9817.
(41) Bardwell, J. C., McGovern, K., and Beckwith, J. (1991) Identification of a protein required for disulfide bond formation in vivo. *Cell 67*, 581−589.
(42) Laue, T. M., Shah, B. D., Ridgeway, T. M., and Pelletier, S. L. (1992) Computer-aided interpretation of analytical sedimentation data for proteins. In *Analytical ultracentrifugation in biochemistry and polymer science* (Harding, S. E., Rowe, A. J., and Horton, J. C., Eds.) pp 90−125, The Royal Society of Chemistry, Cambridge, U.K.
(43) Van Holde, K. E. (1971) *Physical Biochemistry*, 2nd ed., pp 110−136, Prentice-Hall, Inc., Englewood Cliffs, NJ.
(44) Philo, J. S. (1997) An improved function for fitting sedimentation velocity data for low-molecular-weight solutes. *Biophys. J. 72*, 435−444.
(45) Philo, J. S. (2000) A method for directly fitting the time derivative of sedimentation velocity data and an alternative algorithm for calculating sedimentation coefficient distribution functions. *Anal. Biochem. 279*, 151−163.
(46) Parsonage, D., Youngblood, D. S., Sarma, G. N., Wood, Z. A., Karplus, P. A., and Poole, L. B. (2005) Analysis of the link between enzymatic activity and oligomeric state in AhpC, a bacterial peroxiredoxin. *Biochemistry 44*, 10583−10592.
(47) Hawkins, H. C., and Freedman, R. B. (1991) The reactivities and ionization properties of the active-site dithiol groups of mammalian protein disulphide-isomerase. *Biochem. J. 275* (Part 2), 335−339.
(48) Lundstrom, J., and Holmgren, A. (1993) Determination of the reduction-oxidation potential of the thioredoxin-like domains of protein disulfide-isomerase from the equilibrium with glutathione and thioredoxin. *Biochemistry 32*, 6649−6655.
(49) Wunderlich, M., and Glockshuber, R. (1993) Redox properties of protein disulfide isomerase (DsbA) from *Escherichia coli*. *Protein Sci. 2*, 717−726.
(50) Jaeger, J., Sorensen, K., and Wolff, S. P. (1994) Peroxide accumulation in detergents. *J. Biochem. Biophys. Methods 29*, 77−81.
(51) Rouhier, N., Gelhaye, E., Gualberto, J. M., Jordy, M. N., De Fay, E., Hirasawa, M., Duplessis, S., Lemaire, S. D., Frey, P., Martin, F., Manieri, W., Knaff, D. B., and Jacquot, J. P. (2004) Poplar peroxiredoxin Q. A thioredoxin-linked chloroplast antioxidant functional in pathogen defense. *Plant Physiol. 134*, 1027−1038.
(52) Ferrer-Sueta, G., Manta, B., Botti, H., Radi, R., Trujillo, M., and Denicola, A. (2011) Factors affecting protein thiol reactivity and specificity in peroxide reduction. *Chem. Res. Toxicol. 24*, 434−450.
(53) Holmgren, A. (1981) Thioredoxin: Structure and functions. *Trends Biochem. Sci. 6*, 26−29.
(54) Holmgren, A., Ohlsson, I., and Grankvist, M. L. (1978) Thiroedoxin from *Escherichia coli*. Radioimmunological and enzymatic determinations in wild type cells and mutants defective in phage T7 DNA replication. *J. Biol. Chem. 253*, 430−436.
(55) Rouhier, N., Gelhaye, E., and Jacquot, J. P. (2002) Glutaredoxin-dependent peroxiredoxin from poplar: Protein-protein interaction and catalytic mechanism. *J. Biol. Chem. 277*, 13609−13614.

(56) Rouhier, N., Gelhaye, E., Sautiere, P. E., Brun, A., Laurent, P., Tagu, D., Gerard, J., de Fay, E., Meyer, Y., and Jacquot, J. P. (2001) Isolation and characterization of a new peroxiredoxin from poplar sieve tubes that uses either glutaredoxin or thioredoxin as a proton donor. *Plant Physiol. 127*, 1299−1309.
(57) Pedrajas, J. R., Padilla, C. A., McDonagh, B., and Barcena, J. A. (2010) Glutaredoxin participates in the reduction of peroxides by the mitochondrial 1-CYS peroxiredoxin in *Saccharomyces cerevisiae*. *Antioxid. Redox Signaling 13*, 249−258.
(58) Hanschmann, E. M., Lonn, M. E., Schutte, L. D., Funke, M., Godoy, J. R., Eitner, S., Hudemann, C., and Lillig, C. H. (2010) Both thioredoxin 2 and glutaredoxin 2 contribute to the reduction of the mitochondrial 2-Cys peroxiredoxin Prx3. *J. Biol. Chem. 285*, 40699−40705.
(59) Kim, S. J., Woo, J. R., Hwang, Y. S., Jeong, D. G., Shin, D. H., Kim, K., and Ryu, S. E. (2003) The tetrameric structure of *Haemophilus influenza* hybrid Prx5 reveals interactions between electron donor and acceptor proteins. *J. Biol. Chem. 278*, 10790−10798.
(60) Rouhier, N., and Jacquot, J. P. (2003) Molecular and catalytic properties of a peroxiredoxin-glutaredoxin hybrid from *Neisseria meningitidis*. *FEBS Lett. 554*, 149−153.
(61) Reynolds, C. M., Meyer, J., and Poole, L. B. (2002) An NADH-dependent bacterial thioredoxin reductase-like protein in conjunction with a glutaredoxin homologue form a unique peroxiredoxin (AhpC) reducing system in *Clostridium pasteurianum*. *Biochemistry 41*, 1990−2001.
(62) El Hajjaji, H., Dumoulin, M., Matagne, A., Colau, D., Roos, G., Messens, J., and Collet, J. F. (2009) The zinc center influences the redox and thermodynamic properties of *Escherichia coli* thioredoxin 2. *J. Mol. Biol. 386*, 60−71.
(63) Ladner, J. E., Parsons, J. F., Rife, C. L., Gilliland, G. L., and Armstrong, R. N. (2004) Parallel evolutionary pathways for glutathione transferases: Structure and mechanism of the mitochondrial class κ enzyme rGSTK1-1. *Biochemistry 43*, 352−361.
(64) Xia, B., Vlamis-Gardikas, A., Holmgren, A., Wright, P. E., and Dyson, H. J. (2001) Solution structure of *Escherichia coli* glutaredoxin-2 shows similarity to mammalian glutathione-S-transferases. *J. Mol. Biol. 310*, 907−918.
(65) Fernandes, A. P., Fladvad, M., Berndt, C., Andresen, C., Lillig, C. H., Neubauer, P., Sunnerhagen, M., Holmgren, A., and Vlamis-Gardikas, A. (2005) A novel monothiol glutaredoxin (Grx4) from *Escherichia coli* can serve as a substrate for thioredoxin reductase. *J. Biol. Chem. 280*, 24544−24552.
(66) Potamitou, A., Holmgren, A., and Vlamis-Gardikas, A. (2002) Protein levels of *Escherichia coli* thioredoxins and glutaredoxins and their relation to null mutants, growth phase, and function. *J. Biol. Chem. 277*, 18561−18567.
(67) Åslund, F., Berndt, K. D., and Holmgren, A. (1997) Redox potentials of glutaredoxins and other thiol-disulfide oxidoreductases of the thioredoxin superfamily determined by direct protein-protein redox equilibria. *J. Biol. Chem. 272*, 30780−30786.
(68) König, J., Baier, M., Horling, F., Kahmann, U., Harris, G., Schurmann, P., and Dietz, K. J. (2002) The plant-specific function of 2-Cys peroxiredoxin-mediated detoxification of peroxides in the redox-hierarchy of photosynthetic electron flux. *Proc. Natl. Acad. Sci. U.S.A. 99*, 5738−5743.
(69) Parsonage, D., Desrosiers, D. C., Hazlett, K. R., Sun, Y., Nelson, K. J., Cox, D. L., Radolf, J. D., and Poole, L. B. (2010) Broad specificity AhpC-like peroxiredoxin and its thioredoxin reductant in the sparse antioxidant defense system of *Treponema pallidum*. *Proc. Natl. Acad. Sci. U.S.A. 107*, 6240−6245.
(70) Dietz, K. J., Jacob, S., Oelze, M. L., Laxa, M., Tognetti, V., de Miranda, S. M., Baier, M., and Finkemeier, I. (2006) The function of peroxiredoxins in plant organelle redox metabolism. *J. Exp. Bot. 57*, 1697−1709.
(71) Ogusucu, R., Rettori, D., Munhoz, D. C., Soares Netto, L. E., and Augusto, O. (2007) Reactions of yeast thioredoxin peroxidases I and II with hydrogen peroxide and peroxynitrite: Rate constants by competitive kinetics. *Free Radical Biol. Med. 42*, 326−334.
(72) Benesch, R. E., Lardy, H. A., and Benesch, R. (1955) The sulfhydryl groups of crystalline proteins. I. Some albumins, enzymes, and hemoglobins. *J. Biol. Chem. 216*, 663−676.
(73) Kortemme, T., Darby, N. J., and Creighton, T. E. (1996) Electrostatic interactions in the active site of the N-terminal thioredoxin-like domain of protein disulfide isomerase. *Biochemistry 35*, 14503−14511.
(74) Roberts, B. R., Wood, Z. A., Jönsson, T. J., Poole, L. B., and Karplus, P. A. (2005) Oxidized and synchrotron cleaved structures of the disulfide redox center in the N-terminal domain of *Salmonella typhimurium* AhpF. *Protein Sci. 14*, 2414−2420.
(75) Wakita, M., Masuda, S., Motohashi, K., Hisabori, T., Ohta, H., and Takamiya, K. (2007) The significance of type II and PrxQ peroxiredoxins for antioxidative stress response in the purple bacterium *Rhodobacter sphaeroides*. *J. Biol. Chem. 282*, 27792−27801.
(76) Soito, L., Williamson, C., Knutson, S. T., Fetrow, J. S., Poole, L. B., and Nelson, K. J. (2011) PREX: PeroxiRedoxin classification indEX, a database of subfamily assignments across the diverse peroxiredoxin family. *Nucleic Acids Res. 39*, D332−D337.
(77) Atack, J. M., Harvey, P., Jones, M. A., and Kelly, D. J. (2008) The *Campylobacter jejuni* thiol peroxidases Tpx and Bcp both contribute to aerotolerance and peroxide-mediated stress resistance but have distinct substrate specificities. *J. Bacteriol. 190*, 5279−5290.
(78) Hicks, L. D., Raghavan, R., Battisti, J. M., and Minnick, M. F. (2010) A DNA-binding peroxiredoxin of *Coxiella burnetii* is involved in countering oxidative stress during exponential-phase growth. *J. Bacteriol. 192*, 2077−2084.